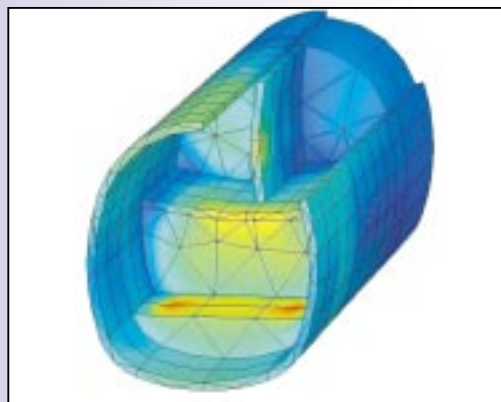


Editorial

In April the newly developed 3D Tunnel program will officially be released . Many months were spent in testing the program, not only at the Delftech park office, but also by a group of Beta testers. The 3D Tunnel program is specifically intended to model tunnels such as shield tunnels (second Heineoord Tunnel, see New Developments) and NATM tunnels. But the 3D Tunnel program allows other 3D situations to be modelled as well, such as the 3D excavation and installation of a diaphragm wall (M. de Kant, see Plaxis Practice). A short description of the 3D Tunnel program is provided in this bulletin.

Last year, in September, a Beta release of the 3D Tunnel program was presented at a users meeting. Besides a lecture on the (theoretical) background of the 3D Tunnel program, a hands-on exercise was given on a simple example problem. Further more it was shown that the PLAXIS 3D Tunnel program is certainly capable of other analyses beyond tunnelling. A case about the indentation of a tractor wheel in soft soil (University of Wageningen) and the excavation of a slurry wall were presented.



Partial geometry of NATM tunnel

Since the release of the Dynamics module last year users have been running dynamic analyses. As this is a new module of Plaxis, many users have to gain experience with it. Therefore, the Plaxis Users Association (NL) organised a well attended 'Dynamics day' with guest speakers Prof. dr. ir. A. Verruijt and T.K. Muller from IFCO. After these interesting lectures, hands-on exercises were conducted in the afternoon to exchange practical experience. Last January, during the course 'Computational Geotechnics' at Berkeley University (USA) a one day Dynamics course was introduced. Some 30 participants from this earthquake sensitive area were present.

The analysis of flexible soil retaining walls is taken a step further. From Blum's analysis and Winkler spring type models to an analysis in Plaxis. The approach of using a Finite Element method with an adequate soil model to analyse flexible soil retaining walls shows that some interesting results can be obtained (Column Vermeer).

Since the Soft Soil Creep model has been implemented, questions have been asked about the role of OCR in the model. A practical example is given and preliminary conclusions are drawn in 'The role of OCR in the SSC model' see Plaxis Practice.

Editorial staff:

Martin de Kant, Plaxis Users Association (NL)
Marco Hutteman, Plaxis Users Association (NL)
Peter Brand, Plaxis bv
Jan Gabe van der Weide, Plaxis bv

Scientific Committee:

Prof. Pieter Vermeer, Stuttgart University
Dr. Ronald Brinkgreve, Plaxis bv

**Bulletin of the
PLAXIS
Users Association (NL)**

**Plaxis bulletin
Plaxis B.V.
P.O. Box 572
2600 AN Delft
The Netherlands
E-mail:
bulletin@plaxis.nl**

IN THIS ISSUE:

Editorial	1
Column Vermeer	1
New developments	4
Improved user services support	7
Recent activities	8
Plaxis Practice	8
The role of OCR	12
Users forum	14
Agenda	16

ON SINGLE ANCHORED RETAINING WALLS

The analysis of flexible soil retaining walls became possible through the work of Blum in the 1930s. Considering single-anchored or single-propped sheet-pile walls, he distinguished between two types of embedments:

- free earth support
- fixed earth support

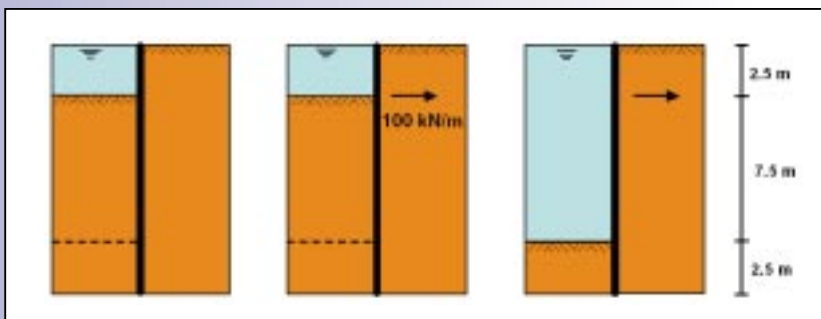
Free earth support implies a relatively short wall with minimum embedment. Fixed earth support implies a somewhat larger embedment. According to Blum's definition, full fixity is achieved when the fixity moment equals the field moment.

Blum's design procedures for retaining walls with free or fixed earth support can be found in most textbooks. In the author's opinion they constitute outstanding contributions to Soil Mechanics. However, as Blum's analysis involves neither the wall stiffness nor the soil stiffness it is bound to be inaccurate. As a consequence, one is now mostly using Winkler spring type models. Unfortunately it is difficult to select appropriate spring constants and I would rather use the FE method. To assess the impact of stiffnesses we decided to perform a series of

*Figure 1
Single-anchored wall with free earth support with 3 stages of construction: first excavation, anchoring and final excavation. In practice anchors will be installed just above the groundwater table.*

	Wall stiffness [EI]	Soil stiffness [E_{soil}] for $\sigma_1 = 100$ kPa
Case A	15 MNm ² /m	45 MPa
Case B	225 MNm ² /m	45 MPa
Case C	225 MNm ² /m	3 MPa

Table 1 Stiffness parameters.



FE-computations. We will consider a single-anchored wall for three different cases.

We considered the geometry of Fig. 1, i.e. an excavation depth of 10 m, an embedment of 2.5 m and an anchor at a depth of 2.5 m. The anchor force was given a fixed value of 100 kN/m.

For all three different cases (A, B and C) the following soil properties were adopted:

$$\gamma' = 10 \text{ kN/m}^3; \quad c' = 2 \text{ kPa}; \quad \phi' = 30^\circ; \quad \delta' = 20^\circ$$

Submerged soil weight was used, as we consider a water table at the soil surface, being not lowered at all, i.e. neither in front nor behind the wall. The excavation was done in three stages of construction:

- 1 Installation of wall and excavation to a depth of 2.5 m
- 2 Application of anchor load of 100 kN/m
- 3 Excavation down to final depth

Hardening soil model: Soil behaviour was simulated using the HS-Model of the Plaxis code. For virgin oedometer loading, this implies an increasing tangent stiffness modulus according to

$$E_{oed} = E_{oed}^{ref} \cdot [(\sigma'_1 + a) / (\sigma'_{ref} + a)]^m \quad \text{with} \quad a = c \cdot \cot \phi$$

where σ'_1 is the major principal stress. We adopted the exponent $m = 0.5$. Within the HS-Model unloading-reloading is described on the basis of Hooke's law. Young's unloading-reloading modulus for increments of stress and strain reads:

$$E_{ur} = E_{ur}^{ref} \cdot [(\sigma'_3 + a) / (\sigma'_{ref} + a)]^m$$

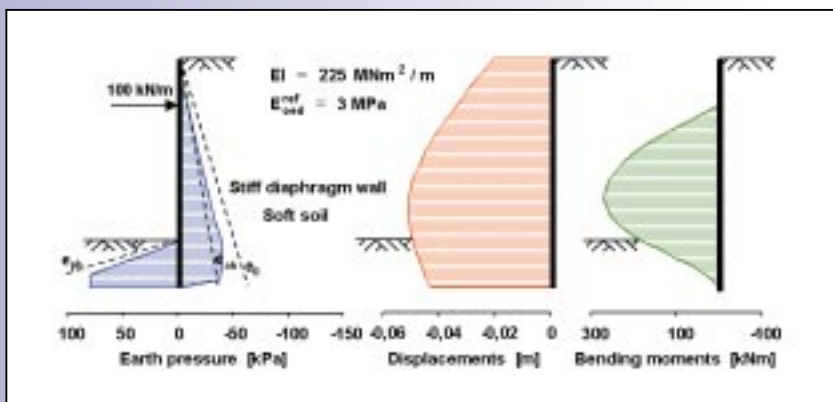
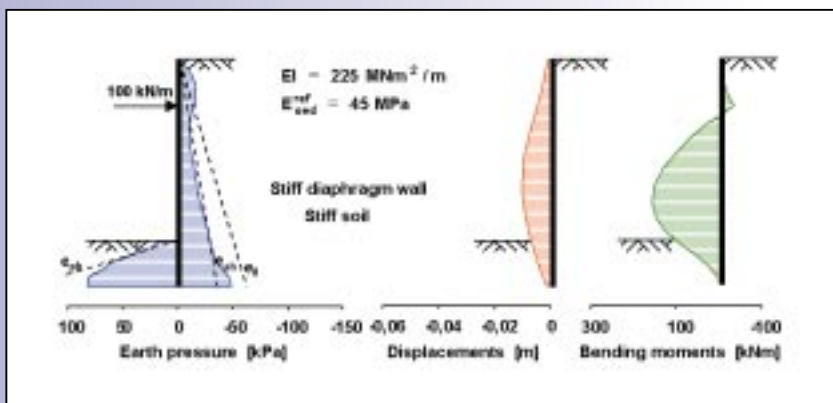
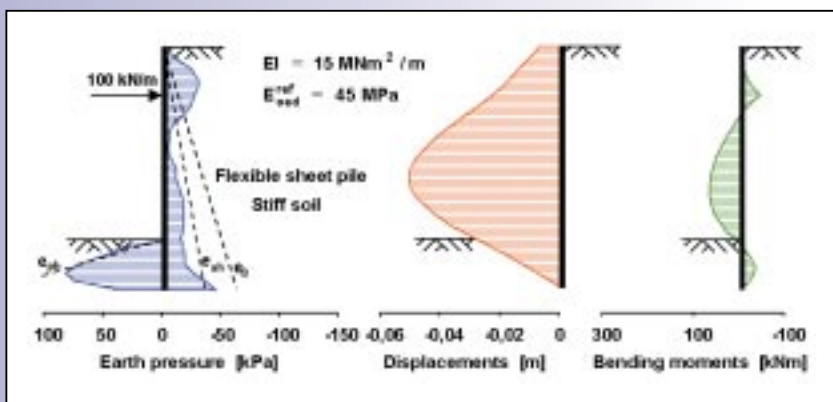
where σ'_3 is the minor principal stress. For all analyses, the over-consolidation ratio was taken to be $OCR = 1.0$ and initial stresses were computed using $K_0 = 0.5$. The HS-Model also allows for a specification of soil stiffness in drained standard triaxial tests. For all analyses, we used

$$E_{50}^{ref} = E_{oed}^{ref} \quad E_{ur}^{ref} = 4 \cdot E_{oed}^{ref} \quad \nu_{ur} = 0.2$$

The only difference between the stiff soil of Cases A and B, and the soft soil of Case C relates to the stiffnesses. The stiff soil is simply a factor 15 stiffer than the soft soil, but the relation $E_{s0} / E_{oed} / E_{ur}$ is 1/1/4 for both soils. Moreover, both the stiff and the soft soil are conveniently given the same strength parameters.

Case A: Considering the FE-results for the combination of a stiff soil and a flexible wall, one observes in Fig. 2a considerable wall bending up to about 5 cm. As a consequence, the active earth pressures reduce significantly; even below the classical minimum of e_{ah} . Indeed, plots of stresses showed significant arching between the anchor and the passive pressure below the bottom of the excavation.

Figure 2
Single-anchored wall
with free earth support.



The simulation of arching behind a flexible wall makes the FEM superior to subgrade reaction type models. In the latter case the spring will yield plastically as soon as e_{ah} is reached and active pressures will never reach smaller values than $e_{ah} = k_{ah} \cdot \sigma'_z$. Fig. 2 clearly demonstrates the significance of arching, as computed active earth pressures are well below the dashed line for e_{ah} . It happens for flexible walls in stiff soils.

Another feature of a wall with low relative stiffness is the fixity of its base. There is a significant fixity moment! Here it should be noted that we computed the embedment length using Blum's design rules for a wall with no fixity at all. Due to the significant amount of arching and the base fixity, computed bending moments are small; approximately half the ones that would follow from Blum's design rule.

Case B: Typical Blum-type results are obtained when considering a stiff wall in a stiff soil (Case B). Below the anchor classical active earth pressures are reached. The passive ones are not fully mobilised, as we designed the wall for a factor of safety of 1.5 on the passive earth pressure. The base of the wall shows no fixity at all and bending moments agree well to the ones that follow from Blum's analytical design procedure. Please note that the same earth pressures and bending moments would have been obtained for the combination of a soft soil and a flexible wall. In such a case we would have the same relative wall stiffness as for the stiff-stiff combination of Case B.

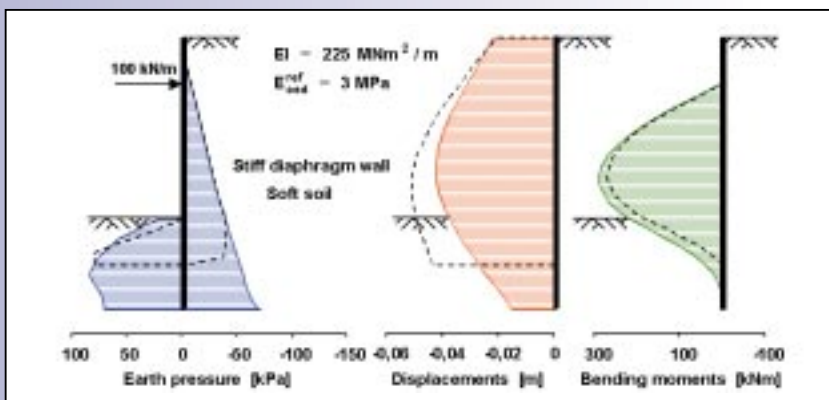
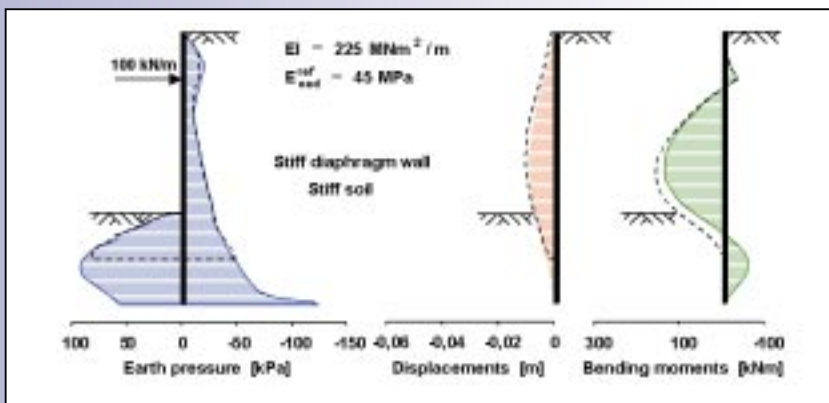
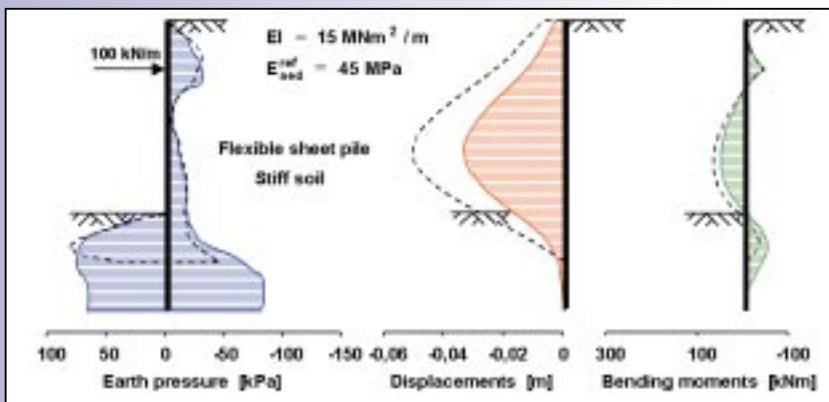
Case C: I was amazed when considering computational results for a stiff wall in a soft soil. Despite the use of a factor of safety of 1.5, the passive earth pressure is nearly completely mobilised. It appears to be caused by an enlarged active pressure. Apparently, the soil is so deformable that wall displacements of about 5 cm are insufficient for a proper reduction of pressure on the active side. As a consequence of the high pressure a bending moment of nearly 300 kNm/m occurs. No doubt, this is well beyond the values that would

follow from Blum's design analysis.

For a stiff wall in soft soil, I would also doubt the results of subgrade reaction type calculations, as this method suffers from the difficulty of selecting proper spring constants. Realistic values would be required both for the active and the passive zone; otherwise it is impossible to predict the high bending moments as obtained for a stiff wall in soft soil.

Figure 3 Single-anchored wall for fixed earth support. Dashed lines indicate results for free earth support.

Embedment: For studying the effect of embedment, we reconsider the wall of Fig. 1, but now the penetration depth is doubled. Hence, instead of 2.5 m, an embedment of



5 m is considered. Following Blum's design rules this would yield full base fixity, such that the fixity moment equals the field moment. Computational results for all three different relative wall stiffnesses are shown in Fig. 3. For comparison, previous data for the shorter wall are indicated by dashed lines.

It appears from Fig. 3 that bending moments are only slightly reduced when increasing wall length. This is surprising as some textbooks suggest a significant effect on the bending moments. Considering present computational data, we conclude that bending moments are in general not significantly reduced by increasing wall penetrations. Present data show, that the reduction of the field moment, as caused by the fixity moment, is more or less compensated by a slight increase of active pressure, as caused by the stiffening of the entire system. Deep penetration is neither of great import when considering displacements. Indeed, a significant reduction of displacements is only achieved for Case A.

Conclusions: When considering a stiff wall in a stiff soil (Case B) typical Blum-type results are obtained. In this case classical active earth pressures will occur, at least below the anchor. Obviously, the passive ones will not be fully mobilised, if the wall is designed for a factor of safety equal of 1.5 on the passive earth pressure, as done in the present example. A flexible wall in a stiff soil (Case A) will result in considerable wall bending and low bending moments. The stiff soil transfers a large part of the active pressure by arching and the flexible wall gets a relative small pressure. A stiff wall in a soft soil (Case C) will result in high active pressures and, as a consequence, high bending moments. Finally we conclude that bending moments are in general not significantly reduced by increasing wall penetrations.

P.A. Vermeer, Stuttgart University

The Plaxis 3D Tunnel program is about to be released. In the previous Bulletin it was explained why this first 3D Plaxis program is devoted to tunnels. At the moment, quite some engineering and research is focused on tunnelling, both NATM and shield or bored tunnelling. Tunnelling involves three-dimensional aspects that cannot be analysed with conventional methods. Hence, there is a demand for a 3D design model for tunnels. Nevertheless, creative users of the Plaxis 3D Tunnel program may find many other applications in addition to the analysis of tunnels.

In the past few months, beta-testers have used a pre-release of the 3D Tunnel program in practical applications. Some of these preliminary results are presented in this

Table 1 Soil layers and parameters used in the Mohr-Coulomb model

Layer	Top m MSL	Type	γ_{unsat} kN/m ³	γ_{sat} kN/m ³	ν	E kN/m ²	c kN/m ²	ϕ °	Ψ °	K_0
1	2.50	Undrained	16.5	17.2	0.34	3900	3.0	27.0	0.0	0.58
2	1.00	Drained	16.5	17.2	0.34	3900	3.0	27.0	0.0	0.58
3	-1.50	Drained	20.5	20.5	0.30	29600	0.0	36.5	6.5	0.47
4	-5.75	Drained	19.0	19.0	0.31	18500	0.0	33.0	3.0	0.47
5	-10.00	Drained	19.5	19.5	0.30	19300	0.0	35.0	5.0	0.45
6	-17.25	Drained	20.5	20.5	0.30	444000	0.0	36.5	6.5	0.50
7	-20.75	Undrained	20.0	20.0	0.32	119000	7.0	31.0	1.0	0.55
8	-25.00	Drained	21.0	21.0	0.30	593000	0.0	37.5	7.5	0.56

Bulletin. In this article I will shortly present some results of a 3D calculation for the Second Heinenoord Tunnel, the first large-scale bored tunnel project under soft soil conditions in the South-West of The Netherlands.

The situation at the Second Heinenoord Tunnel is described in various publications (see References). The tunnel is formed by two tubes with outer diameters of 8.5 m, which were bored under the river Oude Maas. In order to gain experience with tunnel boring under soft soil conditions, the situation was extensively

monitored. Calculations of different construction phases are performed for the North bank. In a 3D finite element model (one symmetric half) the sub-soil, the Tunnel Boring Machine (TBM) and a part of the final lining were modelled according to the 'Grout pressure modelling procedure' (see Fig. 1). The sub-soil was schematised by means of 8 layers, with their location and properties as listed in Table 1. All layers were modelled using the Mohr-Coulomb model. The layers located under the tunnel were given a high unloading stiffness.

The hydrostatic pore pressure distribution for all layers was determined from a phreatic level at +1.0 m.

The 3D finite element model consists of 3440 quadratic volume elements divided over a number of slices (see Fig. 2). Each slice is 3.0 m in the longitudinal tunnel direction. The TBM was modelled over 3 slices and composed of shell (plate) elements, with a flexural rigidity $EI = 50 \cdot 10^3$ kNm²/m, a normal stiffness $EA = 10 \cdot 10^6$ kN/m and a weight $w = 38,15$ kN/m². The radius of the TBM is 4.25 m and its centre point is located at -12.3 m MSL. The 0.35 m thick concrete tunnel lining was modelled using volume elements with the following properties: $\gamma = 24$ kN/m³, $E = 24.6 \cdot 10^6$ kN/m², $n = 0.2$.

The tunnel boring process was modelled according to the 'Grout pressure modelling procedure' as schematised in Fig. 1.

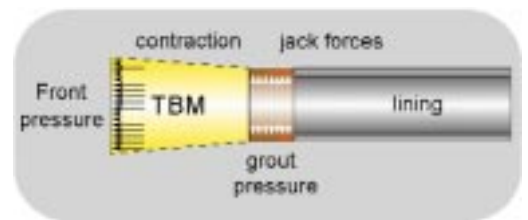


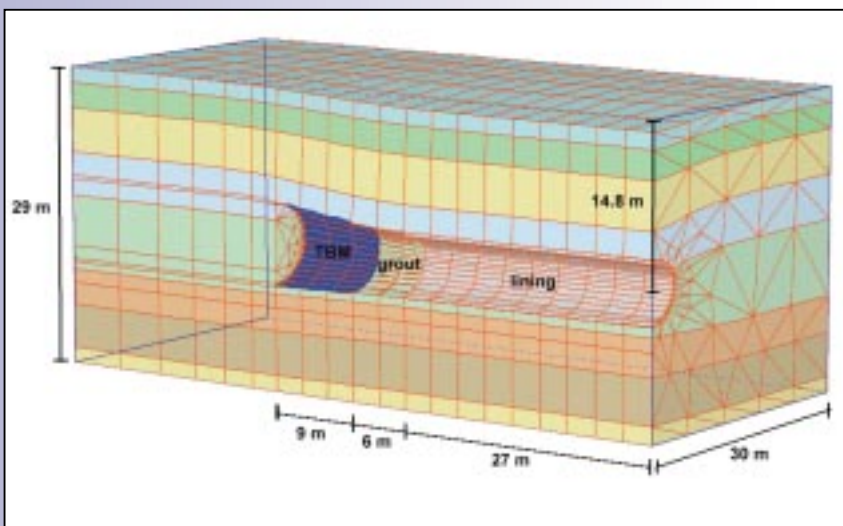
Figure 1 Modelling aspects in 'Grout pressure modelling procedure'.

A front pressure was applied at the bore front to support the soil. The front pressure is 140 kN/m² at the top of the TBM and 259 kN/m² at the bottom. The TBM is conical. The tail

radius is 2 mm smaller than the front radius, which corresponds with a contraction of about 0.48% (0.16% per slice per phase). Behind the TBM grout is injected in the tail void. It is assumed that the grout remains liquified over 2 slices (6 m), which results in a grout pressure on the surrounding soil. The grout pressure is 125 kN/m² at the top and 190 kN/m² at the bottom. Behind the liquified grout zone the tunnel lining is activated and jack forces are applied in backward direction (varying from 3365 kN/m² at the top and 6731kN/m² at the bottom).

In the initial situation, initial stresses are

Figure 2 Deformed mesh at the end of Phase 14 (deformations 50 times enlarged).



m (TBM 3 slices, liquified grout zone 2 slices, tunnel lining 9 slices). The results of the calculation at the end of Phase 14 are presented underneath.

Fig. 2 shows the deformed mesh. This plot clearly shows the settlement trough at the ground surface, with a maximum settlement of about 22 mm. The results are quite realistic and correspond reasonably well to the measurements. This statement also applies to the width of the settlement trough. Calculations using contraction only tend to overestimate the width of the settlement trough, whereas calculations according to the 'grout pressure modelling procedure' give more realistic results. The deformations just above the tunnel lining are somewhat larger than at the settlement surface (max. 38 mm).

Fig. 3 shows the shadings of total displacements. This plot confirms the above and clearly shows where the larger displacements occur (just above the lining). In this plot it can also be seen that the 'buoyancy' of the tunnel is relatively little, since the displacements below the tunnel are small.

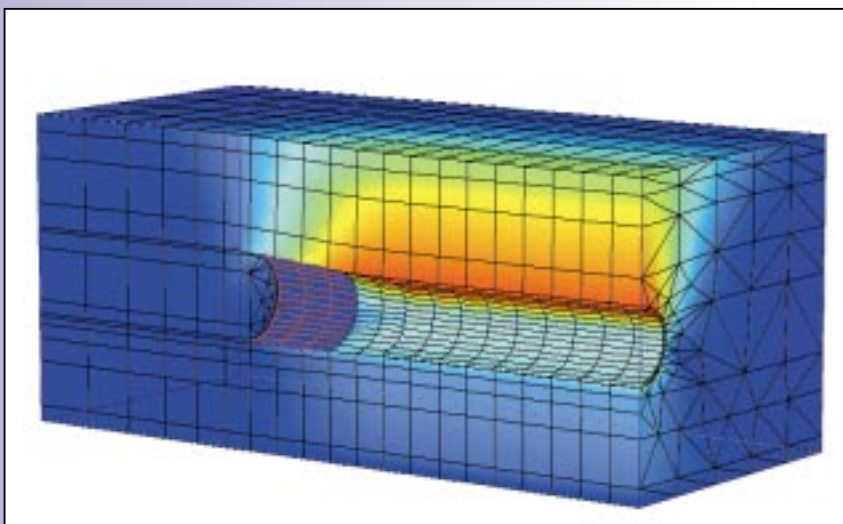


Figure 3 Shadings of total displacement at the end of Phase 14 (displacements 50 times enlarged).

generated by means of the K0-procedure, using K0-values as listed in Table 1. The whole calculation is divided into 14 phases. In Phase 1 the TBM enters the model in the first slice and the process advances 1 slice in each phase. In the final Phase 14 the TBM has advanced 42

In addition to the displacements, the stresses can be visualised in the full 3D mesh as well as in individual and user-defined cross sections. From such plots the three dimensional arching around the tunnel can be viewed. There are also several possibilities to show the forces and deformations of the TBM and the tunnel lining, both in 3D and per cross section. The maximum bending moment in the TBM is around 100 kNm/m and the maximum bending moment in the lining is around 80 kNm/m. These values are also quite realistic.

From the results it can be concluded that it is very well possible to calculate the three dimensional effects around bore tunnels and to accurately predict surface settlements using the grout pressure modelling procedure. The above analysis took some 6 hours to calculate on a Pentium III 500 Mhz with 768 MB RAM.

References:

- [1] Bakker K.J., van Schelt W., Plekkenpol J.W. (1996), Predictions and a monitoring scheme with respect to the boring of the Second Heineoord Tunnel. In: Geotechnical aspects of underground construction in soft ground, (eds: R.J. Mair and R.N. Taylor). Balkema, Rotterdam. pp. 459-464.
- [2] Jaarsveld E.P., Plekkenpol J.W., Messemaeckers van de Graaf C.A. (1999), Ground deformations due to the boring of the Second Heineoord Tunnel. In: Geotechnical infrastructure for transportation infrastructure (eds: F.B.J. Barends, J. Lindenberg, H.J. Luger, L. de Quelerij, A. Verruijt). Balkema, Rotterdam. pp. 153-159.
- [3] CUR / COB (1999), Monitoring bij de Tweede Heineoordtunnel, verslag van een grootschalig praktijkonderzoek naar geboorde tunnels. Final report COB committee K100. CUR / COB, Gouda.
- [4] CUR / COB (1999), 3D Validatie Groutdrukmodel, Meetveld Noord. Report of COB committee L520. CUR / COB, Gouda.
- [5] Bakker K.J. (2000), Soil Retaining Structures; development of models for structural analysis. Dissertation (Delft University of Technology). Balkema, Rotterdam.
- [6] Peters R., Safari B. (2000), 2D Modelling van het tunnelboor- en consolidatieproces. Internal report BSRAP-R-00004, Bouwdienst Rijkswaterstaat, Utrecht.
- [7] CUR / COB (2000), Toetsingsrichtlijn voor het ontwerp van boortunnels voor wegen en railinfrastructuur. Final report COB committee L500. CUR / COB, Gouda.

Ronald Brinkgreve,
DELFT UNIVERSITY OF TECHNOLOGY
& PLAXIS BV

Improved User Support Service

As you may have read in the last Plaxis bulletin, the Plaxis company is growing. Currently the staff consists of 10 people. This means we can further increase the quality and the range of products. In April this will first show by the release of the 3D Tunnel program. Obviously these new products and the increasing group of Plaxis users (now over 2000 professionals !) require good user services. Last year we employed a full time support engineer in order to keep up with the foreseen demand on profession support.

We realise that most support questions occur while working on a project. Obviously such projects have a deadline. Hence, it is important that users can rely on a good adequate HelpDesk. Not only on an operational level, but also on a more scientific level. To ensure urgent questions get the highest priority, we are introducing two different levels of support.

Support service level 1:

This service level is free of charge and provides assistance by e-mail within reasonable response times, obviously depending on the support demand. No telephone and scientific assistance is provided within this service level.

Contact HelpDesk:

e-mail: support@plaxis.nl

Support service level 2:

The second level of support is to users who have a PLAXIS software support agreement. This agreement provides a professional support service on operational as well as on a scientific level, within 24 hours of normal working days.

Contact HelpDesk:

e-mail: support@plaxis.nl

fax: +31 15 2600 451

telephone: +31 15 2600 450

For more information on the support agreement, please contact Plaxis BV.

Recent Activities

Plaxis 3D Tunnel program

As this bulletin shows, the Plaxis 3D Tunnel program is nearly finished. Currently the Plaxis team puts the finishing touch to the 3D Tunnel program and the final release is expected in April this year. The 3D Tunnel program is specifically intended to model shield, bored and NATM type of tunnels. Hence the program has special features such as a state-of-the-art tunnel designer, realistic grout pressure modelling, staged construction, Jointed rock model, etc. The userfriendliness of the input, the automatic mesh generation and robustness of the numerical procedures are in line with the Plaxis 2D software. This means creating the finite element model and prescribing the calculation phases are relatively simple, especially when compared to the efforts it takes using general purpose FE codes. Such codes are usually command driven and lack advanced options needed for the modelling of soil, structures and soil/structure interaction. With this new tool, Geotechnical 3D calculations can become generally applicable.

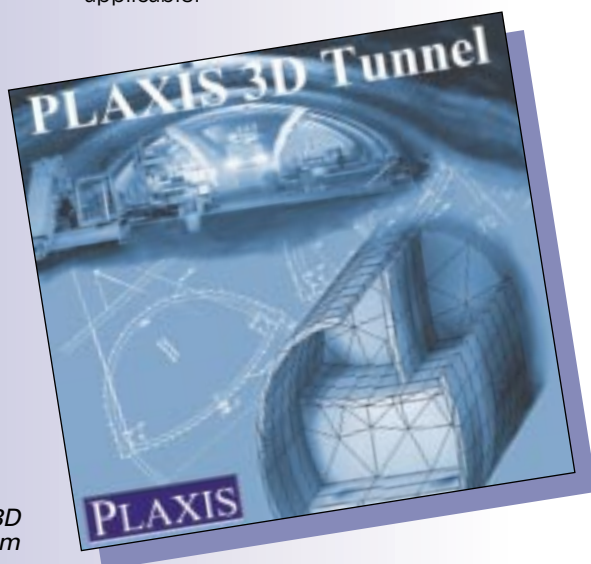


Figure 1 The Plaxis 3D Tunnel Program

Courses

In the past year 11 courses on Computational Geotechnics were lectured at different locations all around the world. Six in Europe, three in Asia, one in the US and one in the Middle East. From the agenda in this bulletin you can see we plan to continue lecturing such

courses. It is also good to realise that the 'local' courses are organised and lectured in cooperation with different local experts, local university professors as well as professionals from the engineering practice. This formula creates tailor made courses, providing theoretical and practical backgrounds on the use of Plaxis. The courses in the Netherlands reflect the Plaxis philosophy with respect to lecturing and the usage of the Plaxis program. The contents of the courses therefor are used as the blue-prints of all international course.

During the past course in Noordwijk, the Netherlands, we welcomed 41 participants from virtually all over the world. Seventeen different nationalities, including people from Japan, Jamaica, Mexico, Brazil, Israel, South Africa, just to mention a few. This is a clear indication of the true International character Plaxis is enjoying.



Figure 2 Participants and lecturers in the Noordwijk course.

So far some 10 new courses have been scheduled for this year. At the upcoming courses in Noordwijk, new lectures dedicated to both Dynamics and 3D modelling are presented (see also Agenda).

Plaxis Practice

RESEARCH PROGRAM ON THE IMPACT OF DIAPHRAGM WALL INSTALLATION. VALIDATION OF A 3D-FE MODEL.

1. Introduction

The North-South metro line in Amsterdam will connect the northern and southern suburbs with the city centre (De Wit, 1998). For reasons of protecting the historic city centre and

restricting the disruption of city life, a bored tunnel will be applied that follows the street pattern as closely as possible and is lowered to a great depth. Consequently the underground stations are at a great depth as well. The stations will be constructed in a building pit with 40m long braced diaphragm walls. One of the most important aspects in the design of the stations is the impact of construction on historical buildings. Because knowledge on the impact of diaphragm wall construction on surrounding buildings is only limited, it was decided to carry out a research project, consisting the following four phases:

- 1 prediction of the impact with a 3D FE-model;
 - 2 full scale test;
 - 3 interpretation of test results;
 - 4 validation of the 3D FE-model.
- This paper focuses on phase four.

2. Full scale test

The test was carried out at the construction site of the Mondriaan Tower, where diaphragm wall panels are applied as foundation elements as well as building pit walls. Figure 1 gives an impression of the test site. During the different stages of construction of 5 panels, a monitoring program was conducted consisting of:

- measurements of vertical and horizontal displacements in the surrounding soil (extensometers, inclinometers);
- settlement and bearing capacity tests on piles;

Fig. 1 Impression of the test-site



- measurements of stress in the trench (piézometers on reinforcement cages).

The geotechnical profile is comparable with the locations of the future stations of the North-South line, see table 1.

Table 1. Geotechnical profile en soil-parameters.

Type of soil	Top level NAP (m)	CPT (Mpa)
Fill (sand)	+2,0	10-15
Clay	-1,0	0,5
Peat	-3,5	0,5
Clay, silt	-7,0	0,5-1,0
Peat	-13,0	1,5
Sand	-14,0 ¹⁾	8-30
Silty sand	-17,0	1-5
Clay (eemklei)	-25,0	1-5
Sand	-28,0	10-30
Silt	-42,0	3

¹⁾ = Foundation layer of ancient buildings on wooden piles

3 FE - validation calculations

The main goal of the validation calculations is developing a model which can be used to predict the soil displacements during the construction of a diaphragm wall. The calibration was carried out, mainly by changing the soil parameters within a certain bandwidth. This calibration procedure has resulted in a "best-fit" calculation (BF). Additionally, calculations were made with the official "North/South-line parameter-set" (NS), which has also been used in the 2D tunnel- and building-pit calculations. In both calculations, BF and NS, the hard-soil model is used.

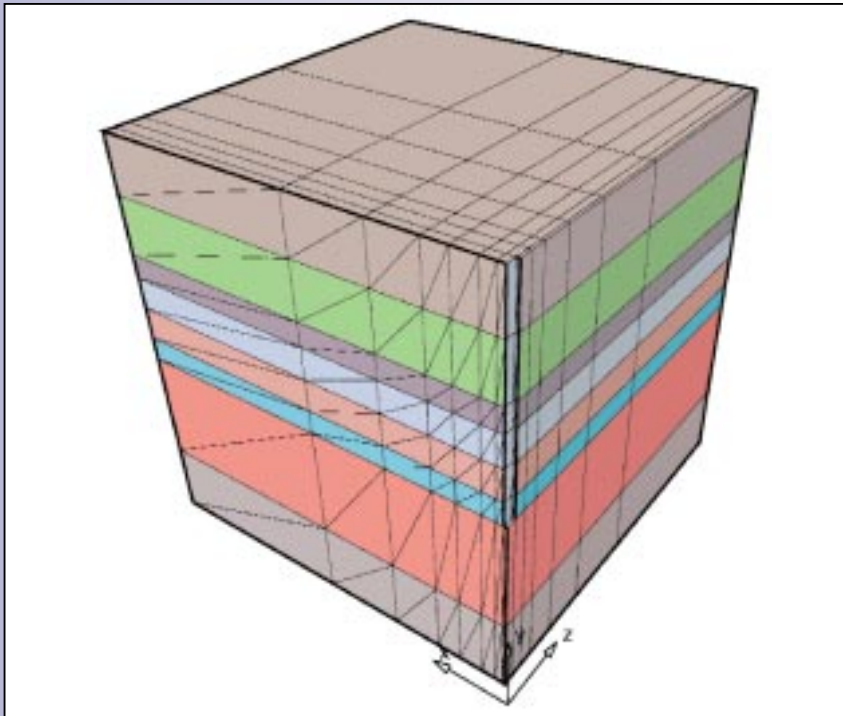
Element mesh and modelling procedure

For the 3D-calculations a preliminary 3D-version of PLAXIS (6.4b) has been used. The mesh is build of 3D-wedge-elements with 15 nodes and 6 Gauss-points. For the calculation of one panel a mesh with approx 5,000 nodes has been used (fig. 2). Only a quarter of the panel is modelled, which means that there are two planes of symmetry: in plan view x- and z-direction.

The construction of a single diaphragm wall panel is modelled using the following stages:

- 1 Excavate the single trench by switching the soil elements off and, simultaneously, applying the bentonite pressure ($\sigma_b = d \cdot \gamma_b$)

Fig. 2 Finite element mesh



is hardened.

Above the hardened concrete, the wet concrete pressure ($\sigma_c = d \cdot \gamma_c$) acts on the faces of the trench ($\gamma_c =$ volume weight of wet concrete). The lateral pressure in step 2 can therefore be described by a bilinear relation:

$$\sigma_h = \begin{cases} d \cdot \gamma_c & \text{for } d \leq h_{crit} \\ (h_{crit} \cdot \gamma_c) + d \cdot \gamma_c & \text{for } d > h_{crit} \end{cases}$$

where h_{crit} is a critical depth which depends on the concrete placing rate, cement type, temperature etc. (Lings et al 1994). In case of a constant rate of concrete placing, γ is equal to γ_b .

During installation the stresses in the soil will initially decrease (stage 1) and, subsequently, increase due to the wet concrete pressure (stage 2). The stresses decrease exponential with increasing distance from the trench. Among these stress-paths the stiffness of the soil varies strongly. The calculations were therefore carried out using non-linear material models: the hard soil model (HSM) and the soft-soil model (SSM). Only the elements representing the clay and peat layers are modelled as undrained.

Calculation results for a single panel

Figure 3 shows the horizontal effective stresses, at a depth of NAP-15m, during the different stages (1 and 2). The initial horizontal stress is about 50 kPa. During excavation the stress at the centre of the panel decreases to about 25 kPa. Due to horizontal load transfer (arching), at the edges of the panel, the stress increases and exceeds K_0 situation. After concreting, the stress at the centre increases significantly. At the corner a decrease of effective stress occurs.

The calculations have shown that load transfer not only acts horizontal but also in vertical direction to relative stiff layers. The displacements in layers beneath those stiff layers therefore decrease and are no longer of influence on displacements of the top layers. Therefore the influence of the panel-depth in a layered subsoil with stiff layers is very small

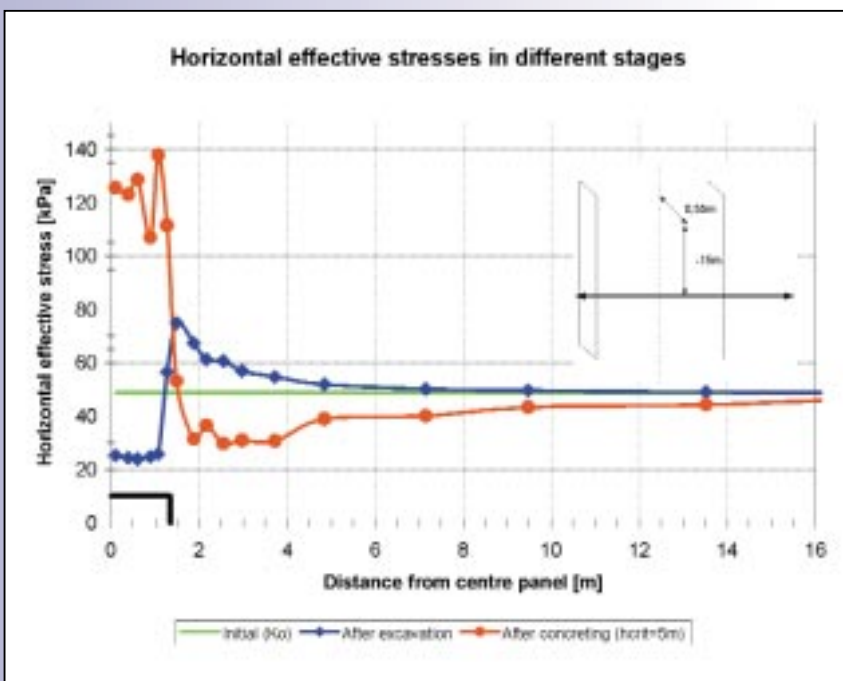


Fig. 3 Horizontal effective stresses in different stages

γ_b) on the faces of the trench ($d =$ depth, $\gamma_b =$ volume weight of bentonite).

- 2 Fill the trench with concrete by increasing the lateral pressure.

Directly after pouring the trench, from bottom up, the lower side of the concrete

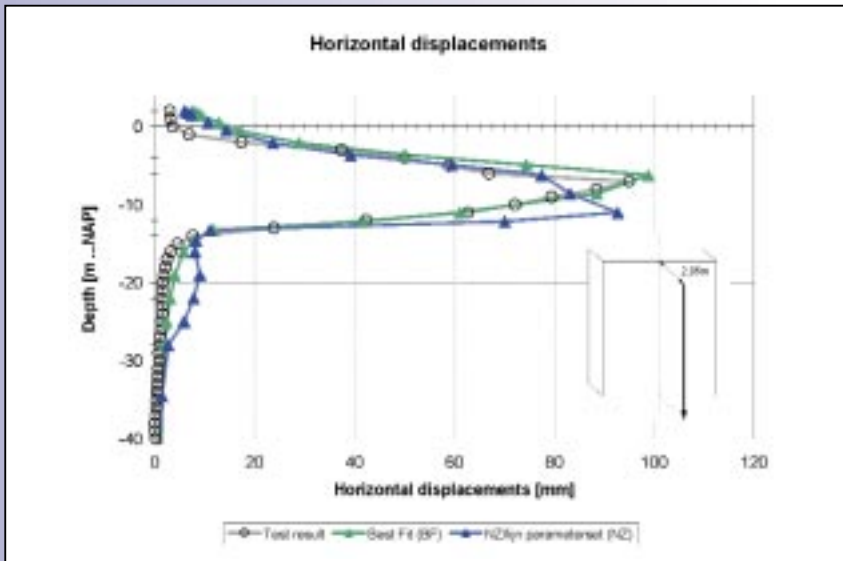


Fig. 4 Horizontal displacements, middle of the panel

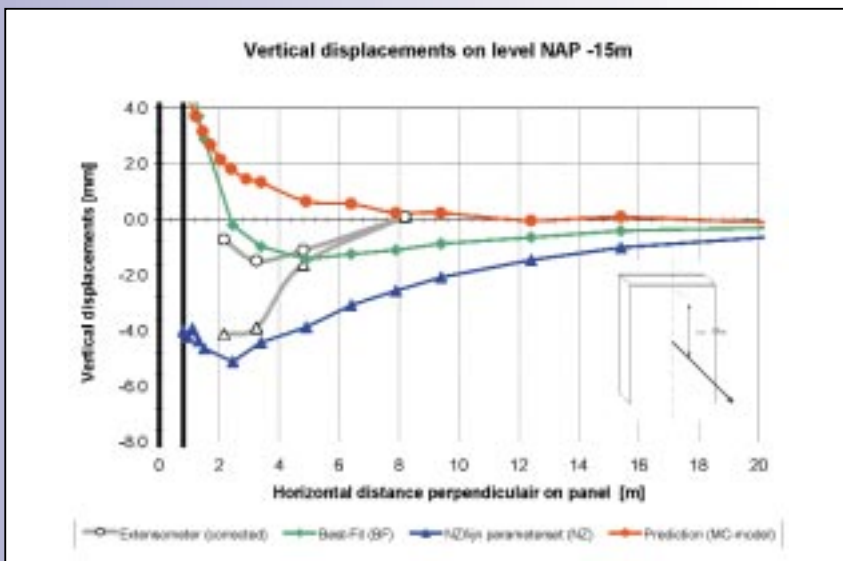


Fig. 5 Vertical displacements on level NAP -15m

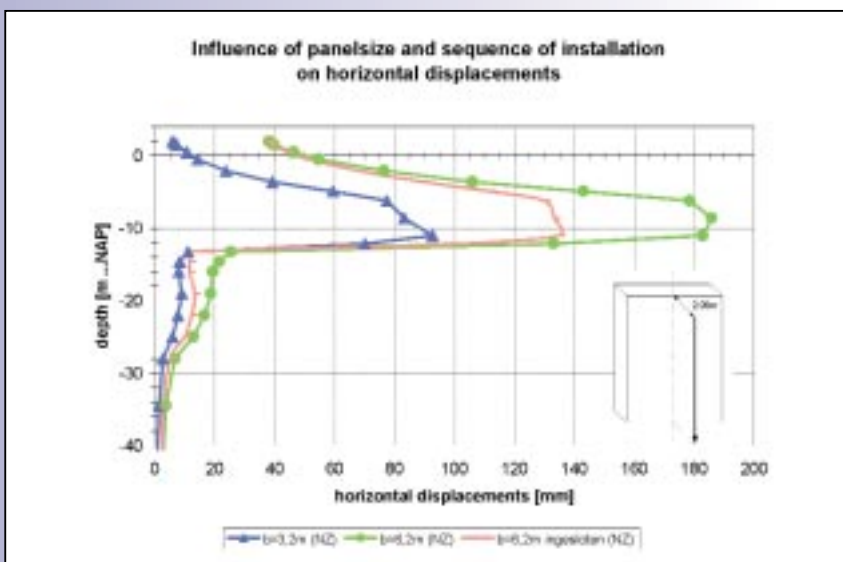


Fig. 6 Influence of panel size and sequence of installation on horizontal displacements

which was an important conclusion of the prediction calculations.

The model was calibrated on the displacements in the concrete-phase (stage 2), because displacements during the excavation phase (stage 1) were too small.

Figure 4 shows the horizontal displacements at the centre of the panel, at approx. 2m from the trench. The maximum displacement occurs in the Holocene top-layers, particularly the peat layer at NAP-6m. The BF-calculation is in good agreement with the test-results. Regarding the top layers, the NS-calculation is also accurate, but the horizontal displacements at lower layers are over predicted. The computed vertical maximum displacements of the sand-layer at a level of NAP-15m (foundation layer of wooden piles) are for both the BF-calculation and the NS-calculation in good agreement with the test-results (fig 5). At the test-site a settlement bowl occurs with a maximum settlement at a distance of 3m from the trench. This is in good agreement with the NZ-calculation, although the calculations show a much wider settlement bowl.

Influence of panel size and installation sequence

At the test-site 5 panels were monitored, with different sizes and shapes. In contrast to the calculations and literature, the panel width was of little influence on the displacements. The reason for this discrepancy has probably been the installation sequence of the panels. The small panel ($b=2,7\text{m}$) was excavated in an undisturbed situation whereas the wide panel ($b=6,4\text{m}$) was excavated between two former installed panels. Those adjacent panels cause a reduction of displacements because of:

- hardening (due to the installation of the adjacent panels the soil is overconsolidated);
- load transfer to adjacent stiff concrete walls.

To confirm this interpretation, the described situation was computed with the calibrated model (NZ-parameters). Figure 6 shows the horizontal displacements of undisturbed panels with different widths, and a wide panel

between to installed small panels. Although hardening was not calculated due to the undrained behaviour, the results are in agreement with the expectation.

Conclusions

The diaphragm wall research project has enlarged the understanding of the impact of D-wall installation on surrounding soil. Main conclusions are:

- the installation of a diaphragm wall in a layered subsoil has no significant impact on nearby wooden pile foundations;
- the ground deformations were relatively small, with exception of the horizontal displacements in the soft top layers;
- the width of a diaphragm wall panel is of great influence on ground displacements. Due to vertical load transfer, the influence of the panel-depth in a layered subsoil with stiff layers, is relatively small;
- the computed displacements with the calibrated 3D-FE model are in good agreement with the test -results.

ing. M. de Kant
Ingenieursbureau Amsterdam
North/South Line Design Office,
Amsterdam, The Netherlands

Literature

Lings, M.L. & C.W.W. Ng. & D.F.T. Nash, 1994, The lateral pressure of wet concrete in diaphragm wall panels cast under bentonite, Proc. Instn. Civ. Engrs. Geotech. Engng, 163-172.

De Wit, J.C.W.M., 1998, Design of underground stations on the North/South line, Proceedings of the World Tunnel Congress, Sao Paolo.

De Wit, J.C.W.M., J.C.S. Roelands & M. de Kant, Full scale test on environmental impact of diaphragm wall trench excavation in Amsterdam, Geotechnical Aspects of Underground Construction in Soft Ground, IS 1999 Tokyo Japan, Balkema Publ.

The role of OCR in the SSC Model

The Over-Consolidation Ratio (OCR) is defined as the ratio between the preconsolidation stress σ_p and the effective in-situ stress: $OCR = \sigma_p / \sigma'_{v\gamma}$. OCR is a state parameter that indicates the amount of overconsolidation of the soil. As long as the effective stress is below the preconsolidation stress, i.e. $OCR > 1.0$, the soil behaviour is stiff. This applies to unloading as well as to reloading. As soon as the existing preconsolidation stress is passed by primary loading of the soil, the soil behaviour is soft, whilst the preconsolidation stress further increases along with the effective stress level. In that case the soil is said to be in a state of normal consolidation, which would imply $OCR = 1.0$. This is exactly what happens in Cam-Clay type of models, like the Soft Soil model in Plaxis.

A similar behaviour can be observed when using the Soft Soil Creep (SSC) model in Plaxis. In that respect the meaning of the OCR-value is similar, although the transition from the stiff reloading behaviour to soft primary loading is more gradual (see Fig. 7.13 of the Plaxis Material Models Manual ^[1]). In order for the preconsolidation stress to 'follow' the effective stress level, time is needed. Hence, when loading the soil very quickly, the OCR-value can (temporarily) become less than 1.0. On the other hand, if the load remains constant, the creep process continues in time, which results in a gradual increase of the preconsolidation stress and OCR (without physical loading). The latter process can be conceived as 'ageing'. The idea that ageing would lead to an increase of the preconsolidation stress was introduced by Bjerrum in his creep formulation ^[2]. This idea is also adopted in the SSC model. In the SSC model the increase of the creep strain in time

(= creep strain rate) depends (in addition to the modified creep index, μ^*) on the ratio of the effective stress and the preconsolidation stress, i.e. on the inverse of OCR. Hence, starting from an initial effective stress state, the initial creep strain rate depends on the initial OCR-value.

The latter is not very known among Plaxis users. Since practical situations always involve effective stresses from the very beginning, the creep process (settlement) starts immediately without additional loading, whereas the 'settlement velocity' depends on the OCR-value. For reasonable combinations of SSC parameters, the use of a default initial OCR-value of 1.0 in the K_0 -procedure may lead to excessive initial settlement velocities. Hence, the initial OCR-value needs to be selected with care. An initial OCR-value larger than 1.0 is generally recommended.

It is generally said that for 'normally consolidated soils' (like the soft clays in the

west of The Netherlands) the initial OCR-value is, per definition, equal to 1.0. On the other hand, even very soft soils often show a preconsolidation stress that is over 20 kPa beyond the in-situ stress level. Particularly in the top layer (just below the ground surface) crust forming may occur, which is associated with relatively stiff and strong behaviour. The reason for this can be drying of the soil, variations of the phreatic level, temporary loads, temperature changes, etc. Nevertheless, these soil are still considered to be 'normally consolidated', but the actual OCR-value is often higher than 1.0.

Let us consider, for example, a 10 m thick clay layer under standard boundary conditions with properties as listed in Table 1. The parameters are arbitrary, but realistic for a normally consolidated clay. Initial stresses are generated with the K_0 -procedure, using different initial values of OCR (OCR_0). On using different OCR_0 -values, Plaxis proposes different K_0 -values, but all K_0 -values are reset to their original value of $K_0^{nc}=0.703$. For all values of OCR_0 a drained calculation is performed for a total time of 1000 days, just to let the soil creep under its self weight without additional loading. The results of these calculations are presented in Fig. 1.

From Fig. 1 it can be seen that there is a remarkable difference in settlement, which is particularly caused by the initial inclination of the time-settlement curve, i.e. the initial creep rate. For $OCR_0=1.0$ the initial creep rate is quite unrealistic. Considering rather soft 'normally consolidated' soils, it is quite realistic to have a settlement of 0.05 m a year, decreasing down to 0.01 m a year when the soil hasn't been disturbed for a some years. In the above situation this is well reflected by the choice of $OCR_0=1.4$. At $t=1000$ days the inclination of all curves is almost the same, except for $OCR_0=2.0$, which would suggest that the actual OCR's have increased to almost the same value. Evaluation of the actual OCR-values at $t=1000$

Figure 1:
Time-settlement curves
for different initial
values of OCR

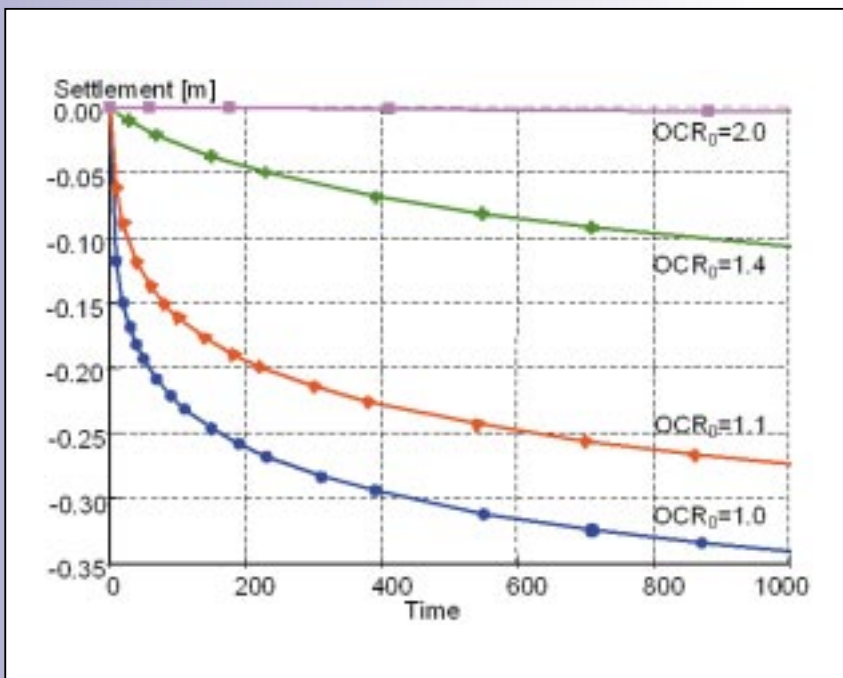


**Table 1. Properties of arbitrary clay layer,
modelled with the Soft Soil Creep model**

γ_{wet}	κ^*	λ^*	μ^*	ν	c	ϕ	ψ	K_0^{nc}
17	0.02	0.10	0.005	0.15	1.0	26.0	0.0	0.70

kN/m³

days gives $OCR \approx 1.8$ for all cases, except for $OCR_0 = 2.0$. In the latter case OCR has hardly increased.

From the above results it could be concluded that an initial OCR-value of 1.4, to be used in the K_0 -procedure, would be a good choice. This could indeed be said for the above example and perhaps for other cases, but it cannot be stated in general. It is a good habit for a practical application to simulate a certain creep period in a drained calculation without additional loading and to evaluate the initial OCR-value. Please note that when using initial OCR-values larger than 1.0, Plaxis will propose $K_0 > K_0^{nc}$, whereas for 'normally consolidated soils' it is recommended to reset $K_0 = K_0^{nc}$. If the resulting settlement velocity is too high and the other parameters of the SSC model have been properly determined, then the initial value of OCR should be increased (or the modified creep index μ^* should be reevaluated).

In conclusion, the initial OCR-value in the Soft Soil Creep model needs to be selected with care. In principle, the initial value depends on the ratio between the initial preconsolidation stress and the effective in-situ stress (which is generally slightly larger than 1.0), but it should be realised that the initial OCR-value also determines the initial settlement velocity. A first estimate could be $OCR = 1.4$, but it is advisable to simulate the creep process and adapt OCR if necessary.

RONALD BRINKGREVE,
DELFT UNIVERSITY OF TECHNOLOGY
& PLAXIS BV

References

- [1] Brinkgreve R.B.J., Vermeer P.A. (1998), PLAXIS Finite Element Code for Soil and Rock Analysis, Version 7, Part: Material Models Manual. Balkema, Rotterdam
- [2] Bjerrum L. (1967), Engineering geology of Norwegian normally consolidated marine clays as related to settlements of buildings. Géotechnique 17 (2), pp. 81-118.

Users Forum

Question:

I have some difficulties in generating the initial stresses in my project. My project is a tunnel 200.0 m underground and is not including the ground surface; otherwise the model will be too big. Therefore, the initial stresses at the top of the model are not zero and should include the overburden above the top of the model. Could you please give me a hint solving this problem?

Answer:

If the model becomes too large you can eventually omit the upper part, but you have to compensate for the missing soil weight otherwise non-realistic stresses will be generated. To include an overburden pressure you have to do the following: Create a thin layer with thickness h at the top of your model representing the omitted soil (see Figure 1). The weight of the soil in the thin layer is higher than the omitted soil and equal to $(\gamma_{virtual} = \gamma_{real} * h_{real} / h_{virtual})$. For example in Figure 1, $(\gamma_{virtual} = 18.0 * 130.0 / 1.0 = 2340.0 \text{ kN/m}^3)$. In this way you can generate realistic initial stresses by means of the K_0 procedure.

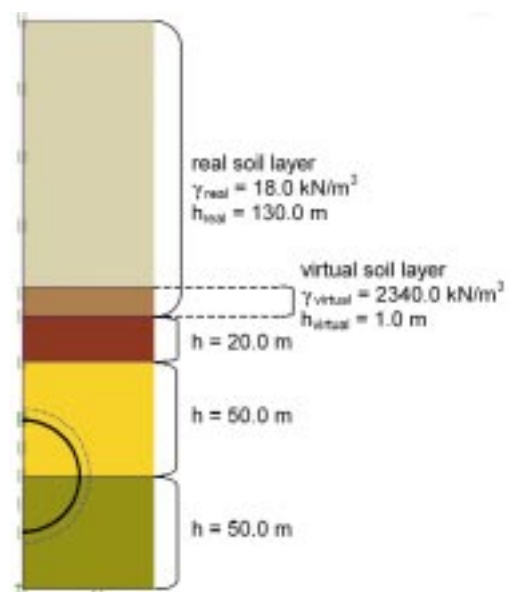


Figure 1: Replacement of 130.0 m of soil by 1.0 m of soil with a higher density.

Question:

Why are the stresses of non-porous materials not shown and how can I visualise them anyway?



Answer:

Non-porous material is general used for structural purposes like concrete, and stresses can therefore become quite large. As a result, stresses in the soil cannot be viewed in detail. By excluding the stresses in structural elements, the soil stresses remain clearly visible. The stresses in non-porous material are calculated though and can be viewed in tables and cross-sections.

However, there is a trick to view the stresses in non-porous material:

Calculate the problem and if all the calculations are finished and you want to have a look at the stresses in output then save the calculation data by pressing the save icon. Then go directly to Input and open the concrete material data set. Change <non-porous> to <drained> and exit the material data set. Save the Input data and go directly to Output by pressing the Output icon. In Output the stresses in the non-porous material set are now visible. Output is tricked in believing that the non-porous material set is drained and shows the stresses.

ACTIVITIES

03-06 JANUARY, 2001

Short course on Computational Geotechnics (English)
One day Dynamics course included
Berkeley, California, U.S.A.

22-24 JANUARY, 2001

Course on Computational Geotechnics (English)
Noordwijkerhout, The Netherlands

19-21 MARCH, 2001

Course on Computational Geotechnics (German)
'Finite Elementen Anwendungen in der Grundbaupraxis'
Stuttgart, Germany

20-22 MARCH, 2001

Short course on Computational Geotechnics (English)
Kuala Lumpur, Malaysia

26-28 MARCH, 2001

International course for experienced Plaxis users (English)
Noordwijkerhout, The Netherlands

02-04 APRIL, 2001

Course on Computational Geotechnics (English)
'Numerical methods in Geotechnical Engineering'
Eynsham Hall, Oxfordshire, United Kingdom

23-25 APRIL, 2001

Short course on Computational Geotechnics (Arabic/ English)
Cairo, Egypt

06-09 AUGUST, 2001

Short course on Computational Geotechnics (English)
One day Dynamics course included
Boulder, U.S.A.

27-31 AUGUST, 2001

XVth ISSMGE International Conference on Soil Mechanics and Geotechnical Engineering (XV ICSMGE)
Istanbul, Turkey

01-03 SEPTEMBER, 2001

Post-conference event (XV ICSMGE)
Short course on Computational Geotechnics (English)
Istanbul, Turkey

WINTER, 2001

Short course on Computational Geotechnics (French)
'Pratique des éléments finis en Géotechnique'
Paris, France

20-23 JANUARY, 2002

Course on Computational Geotechnics (English)
Noordwijkerhout, The Netherlands

24-27 MARCH, 2002

International course for experienced Plaxis users (English)
Noordwijkerhout, The Netherlands

For more information on these activities please contact:

Plaxis bv
P.O. Box 572
2600 AN
DELFT
The Netherlands
Tel: +31 15 26 00 450
Fax: +31 15 26 00 451
E-mail: info@plaxis.nl